Supplementary Material (ESI) for Chemical Communications

Experimental Section.

Materials. ClCN was prepared according to the published procedure[8] and purified by vacuum distillations. BrCN (97 %, Aldrich) and ICN (Aldrich) were used as received. The mixture of $S_4(AsF_6)_2$ and $S_8(AsF_6)_2$ (1 : 1 ratio) was prepared according to the previously published account[9]. SO_2 (Liquid Air, 99.9998 %) was distilled onto CaH_2 and stored for at least 24 h prior to use.

General procedures. All reactions were performed in two-bulb, two-valve Pyrex vessels incorporating 25 ml bulbs using techniques that have been described previously[10]. Solid reagents and crystals were manipulated in a Vacuum Atmospheres Dri-Lab equipment with a Dri-Train (HE-493) and 1 kg of 3 Å molecular sieves contained in an internal circulating drying unit. FT-IR spectra of Nujol mulls between KBr disks were recorded on a Thermo Nicolet FT IR 470 spectrometer (32 scans, resolution 2.0 cm^{-1}). FT-Raman spectra were recorded at 293 K on a Bruker IFS66 FT-IR equipped with a Bruker FRA106 FT-Raman accessory using a Nd: YAG laser (emission wavelength, 1064 nm; maximum laser power, 3009 mW; used laser power 5.5 %). Samples were sealed in melting point capillaries, and data were collected in the backscattering mode (180^o excitation; resolution 2.0 cm^{-1}). Elemental analyses were obtained from Galbraith Laboratories. Inc., Knoxville, Tennessee. The molecular geometries optimizations, vibrational frequency calculations were performed at the (U)MPW1PW91 level of theory employing the 6-311G+(2df) (**1(Cl)**$^{+\bullet}$ and **1(Br)**$^{+\bullet}$) and STO-3G (**1(I)**$^{+\bullet}$) basis sets using Gaussian03 suite of program[11] (fig. S5). Dimers [**1(Cl)**]$_2$, $[S_3N_2^{+\cdot}]_2$ and [HCNSSN]$_2$ were optimized for closed shell S = 0 (MPW1PW91/6-31G**) state with the appropriate symmetry constraints using experimental solid state geometries as inputs. The optimized geometries were minima as indicated by the absence of imaginary frequencies. Single point CASSCF(6,6)/6-31G** calculations of S=1 and S=0 states of [**1(Cl)**]$_2$, $[S_3N_2^{+\cdot}]_2$ and [HCNSSN]$_2$ dimers were performed using the geometry of the corresponding DFT optimized closed shell S=0 state.

Vibrational frequencies of **1(Cl)**$^{+\bullet}$, **1(Br)**$^{+\bullet}$, and **1(I)**$^{+\bullet}$ were animated and assigned using MOLEKEL[12] and are listed in table S1.

EPR Instrumentation. The EPR experiments were performed using a commercial Bruker EMX spectrometer consisting of a Varian electromagnet, X-band (9.8 GHz) microwave bridge in conjunction with a Bruker 4102 ST/9514 rectangular resonator with nitrogen-gas flow cryostat. The temperature was varied in the range from 340 K to 140 K (±1 K) by an Oxford instrument auto-tuning temperature controller. The S-band (3.4 GHz) and K-band (24.5 GHz) EPR spectra were recorded using a commercial ESP Bruker spectrometer with microwave bridges in conjunction with Bruker dielectric resonators ER 4118 SPT-NI and ER 6706 KT, respectively. The ESP300E spectrometer was equipped with helium cryostat. The temperature was controlled by helium flow an Oxford instrument auto-tuning temperature controller ITC504.

Simulation of EPR spectra. The EPR powder spectra have been analysed using commercial Bruker programs WINEPR to extract basic spectral parameters and XSophie for simulation and fitting of spectra with anisotropic *g*-factors and dipolar coupling tensor *D*. Simulated separated doublet and triplet spectrum were added together using simple

routine write in MATLAB. The triplet state is described by a dipolar coupling tensor *D* that can be parameterized in terms of two Zero Field Splitting parameters, *D* and *E*. The magnitude of |*D*| is a measure of the delocalization of the molecular orbitals involved in the triplet state and is inversely proportional to the cube of the distance between the unpaired electrons. The magnitude of the second ZFS parameter |*E*| is attributed to the extent of distortion from axial symmetry and lies in the range $0 \leq 3|E|/|D| \leq 1$, where the extremes represent axial ($|E| = 0$) and orthorhombic symmetry ($3|E|/|D| = 1$).

Synthesis of $BrCNSSSAsF_6$ (2(Br)). 0.7326 g (0.0006427 moles) 1 : 1 mixture $S_4(AsF_6)_2$ and $S_8(AsF_6)_2$ was loaded into one bulb of a two-bulb vessel. The vessel evacuated and the valve to the bulb containing sulfur cations mixture closed. 0.2963 g (0.002795 moles) BrCN was condensed to the second bulb followed by 15.65 g of SO_2 forming a clear transparent solution. This solution was poured onto sulfur cations mixture in 5 portions with stirring during 5 hrs, then the mixture was left stirring for additional 12 hours. The end of the reaction was indicated by the presence of red solution over a black-green precipitate. The solution was filtered to the second bulb, SO_2 slowly condensed back (7-8 times) until all the green solid was completely transferred to the second bulb forming green shiny crystals. A very small amount (about 10-20 mg) of white-brown powder (supposedly 1,2,4-thiadiazol) remained in the first bulb as an insoluble part. Black-green microcrystalline solid formed in the second bulb was recrystallized from SO_2 3 times till it turned dark-green giving 0.470 g (47 % yield based on sulfur cations) of pure $BrCNSSSAsF_6$. The solubles from recrystallization (0.412 g) were further purified giving additional 0.217 g of pure $BrCNSSSAsF_6$, thus increasing the yield to 68 % (based on sulfur cations). Elemental analysis, found/calc., %: C, 3.19/3.07 ; N, 3.87/3.58; S, 23.40/24.60; F, 28.96/29.15; Br, 20.12/20.43. IR and Raman frequencies along with the assignments are listed in table S1. The ESR spectrum of a 10^{-2} M solution of $BrCNSSSAsF_6$ in SO_2 consisted of one singlet with g = 2.0167.

Synthesis of $ICNSSSAsF_6$ (3(I)). 0.860 g (0.000755 moles, 49 % excess) 1 : 1 mixture $S_4(AsF_6)_2$ and $S_8(AsF_6)_2$ was loaded into one bulb of a two-bulb vessel. The vessel evacuated and the valve to the bulb containing sulfur cations mixture closed. 0.235g (0.00153 moles) ICN was condensed to the second bulb followed by 12.561 g of SO_2 forming a clear slightly pink (due to traces of I_2) solution. This solution was poured onto sulfur cations mixture in 7 portions with stirring during 4.5 hrs. SO_2 was slowly evaporated to the second bulb, during which process a green-black zone formed on the sides of the bulb and a black residue formed at the bottom of the bulb. A green-black product (0.40 g, crude $ICNSSSAsF_6$) was collected from the sides ("the 1st crop"). The remaining residue at the bottom (0.71 g) was reacted further with additional 0.0508 g (0.000332 moles) ICN added in 5 portions with stirring during 2.5 hrs. After recrystallization and washing the residue with a small amount of SO_2 4 times, 0.32 g of crude brown-green solid was collected ("the 2nd crop"). First and second crops (0.40 g and 0.32 g respectively) were joined together and recrystallized from SO_2 several times after that 300 mg (37 % yield, based on ICN) of reasonably pure green crystalline $ICNSSSAsF_6$ recovered. Elemental analysis, found/calc., %: C, 2.87/2.74 ; N, 3.38/3.20. IR and Raman frequencies along with the assignments are listed in table S1.

The soluble material (0.75 g in total), which contained an excess sulfur cations and hydrolysis and oxidation by-products as well as small amount of $ICNSSSAsF_6$, was

reacted with 0.0998 g (0.000652 moles) ICN during 12 hrs producing a red-brown solution over a white-brown precipitate (supposedly 1,2,4-thiadiazol) but no additional amount of ICNSSSAsF_6 isolated.

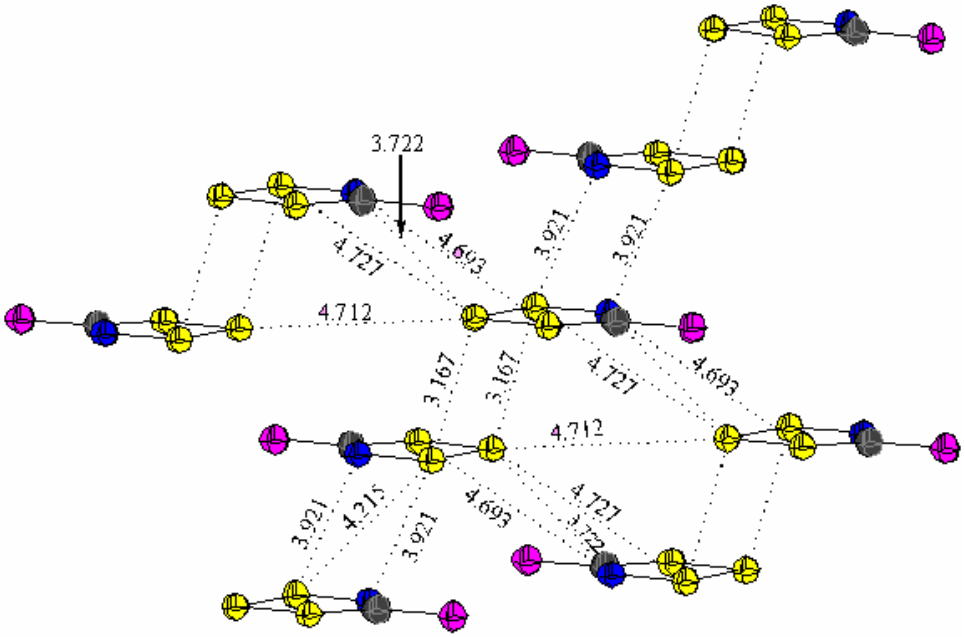

Fig. S1. Packing diagram of [**1(Cl)**][AsF_6] with the nearest interdimeric contacts illustrated.

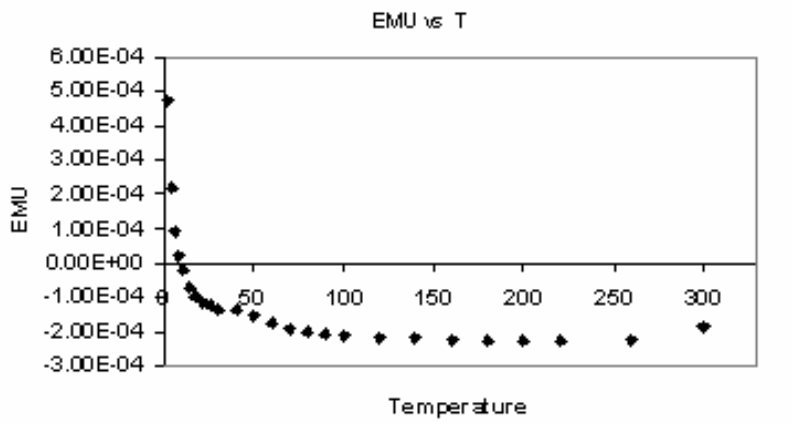

Fig. S2. Temperature dependence of magnetic susceptibility of **1(Cl)**AsF_6.

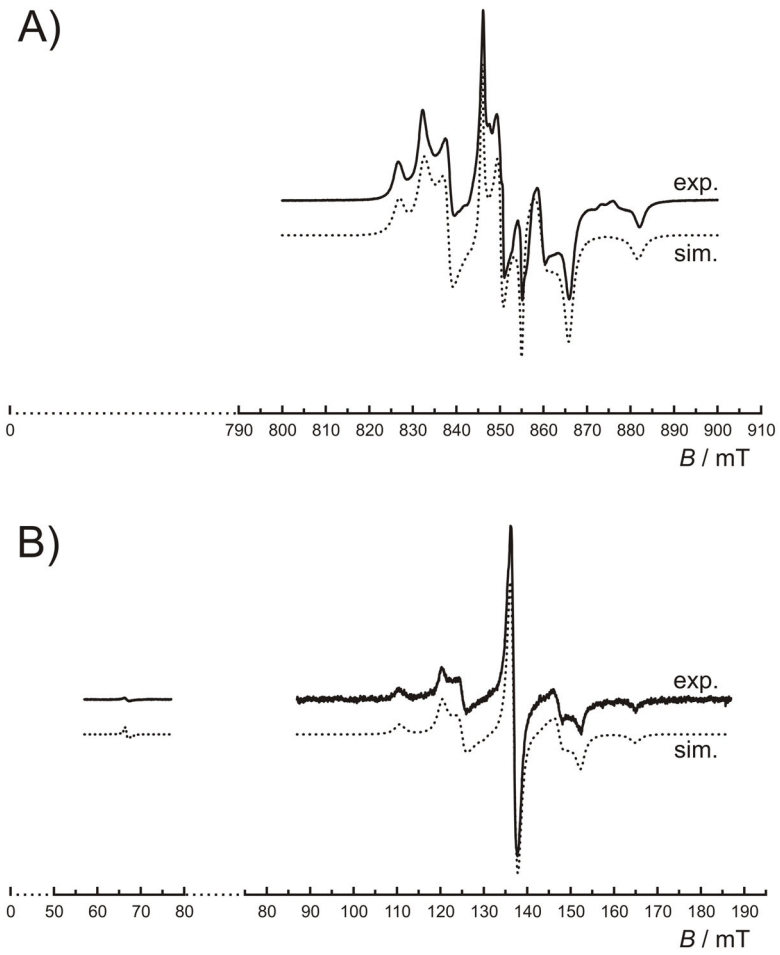

Fig. S3. Room temperature EPR spectra of a powdered sample of $[ClCNSSS^{+\cdot}]_2[AsF_6^-]_2$. A) Experimental (solid line) and simulation (doted line) spectra at K-band; B) experimental (solid line) simulated (doted line) spectra at S-band.

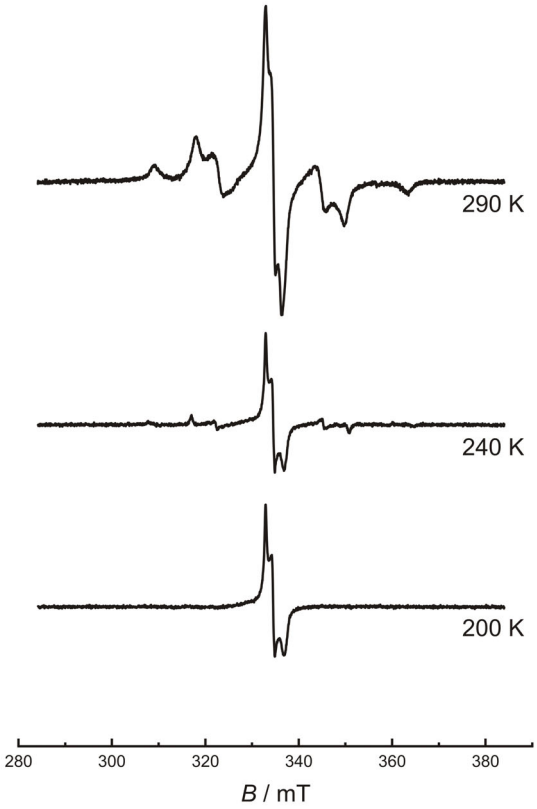

Fig. S4. Representative EPR spectra of [**1(Cl)**]$_2$[AsF_6]$_2$ at 200, 240 and 290 K.

Table S1. Experimental and calculated vibrational frequencies for **1(Cl)**$^{+\bullet}$, **1(Br)**$^{+\bullet}$ and **1(I)**$^{+\bullet}$.

ClCNSSSAsF$_6$ (**1(Cl)**AsF$_6$)			BrCNSSSAsF$_6$ (**1(Br)**AsF$_6$)			ICNSSSAsF$_6$ (**1(I)**AsF$_6$)			
IR	Raman	Calc. (IR,Raman)	IR	Raman	Calc. (IR,Raman)	IR	Raman	Calc. (IR,Raman)	Assignment
	1493(7)						1679(3)		?
over-lapped	1477(23)	1553(190, 34)	over-lapped	1472(38)	1544(179, 39)	over-lapped	1446(35)	1387(186, 84)	ν_s(CN)
	14??								
957m	959(4)	996(76,3)	890m	891(4)	927(30,4)	842m	841(4)	859(45,20)	ν_{as}(CN) ip
841m	842(2)	882(96,<1)	819mw		857(103,<1)	787m	791(1)	743(2,4)	ν_s(SN)
708s	710(6)		709s	710(5)		709s	708(3)		ν_3(AsF$_6$)
670m	674(12)		671m	674(9)		668s	672(5)		ν_1(AsF$_6$)
615w	618(16)	624(7,17)	616w	619(11)	625(8,16)	611ms	615(13)	595(5,24)	ν_s(CS)
555w	558(2)		557w	559(2)		558m			ν_2(AsF$_6$)
530vw	530(68)	539(2,18)	523w	523(85)	531(2,27)	512m	512(80)	569(2,40)	ν_s(S_1S_2)
517vw		540(1,0)	500vw		522(1,0)			455(2,0)	δ(CN) o.o.p
458sh	465(15)	457(5,10)			416(3,9)	446w		385(3,8)	ring def. i.p.
435sh	442(14)	453(7,17)	453vw	459(13)	450(7,15)	484w	446(7)	496(5,6)	ν_s(S_2S_3)
393s	400(2)		395s	406(12)		397vs	397(11)		ν_4(AsF$_6$)
	369(4)			369(3)			367(2)		ν_5(AsF$_6$)
	354(11)	359(<1,8)		284(13)	289(2,6)		233(9)	228(2,4)	ν(C-X)
	255(10)	245(<1,4)		241(7)	191(<1,2)			161(<1,5)	ring twist i. p.
	151(25)	219(2,0)		205(10)	204(2,0)		172(10)	198(2,0)	δ(CNS) o.o.p.
	122(38)	106(0,<1)		148(43)	102(0,<1)		142(30)	102(0,<1)	ring def. o.o.p.
				116(60)					?

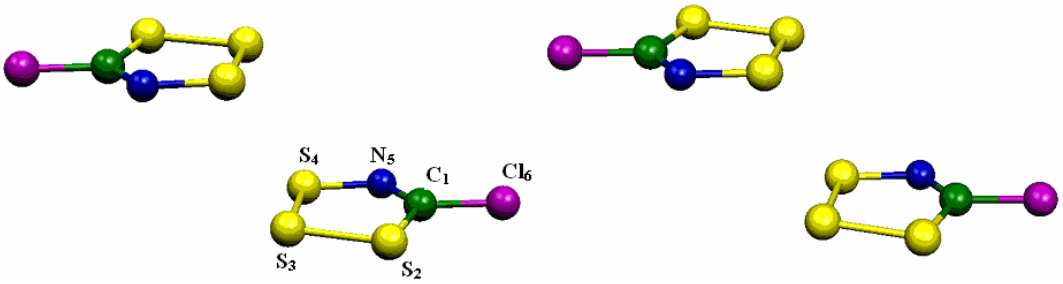

Fig. S5a. Calculated (left) and solid state (right, RT) geometries of $[ClCNSSS]_2^{2+}$ at MPW1PW91/6-31 G* level of theory. Calculated and experimental bond distances and intradimer contacts are listed in table S2.

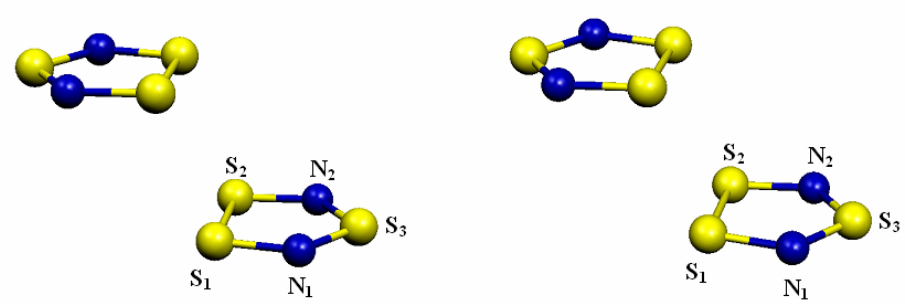

Fig. S5b. Calculated (left) and solid state (right, SO_3F-salt[14]) geometries of $[S_3N_2]_2^{2+}$ at MPW1PW91/6-311+ G(2df) level of theory. Calculated and experimental bond distances and intradimer contacts are listed in table S2.

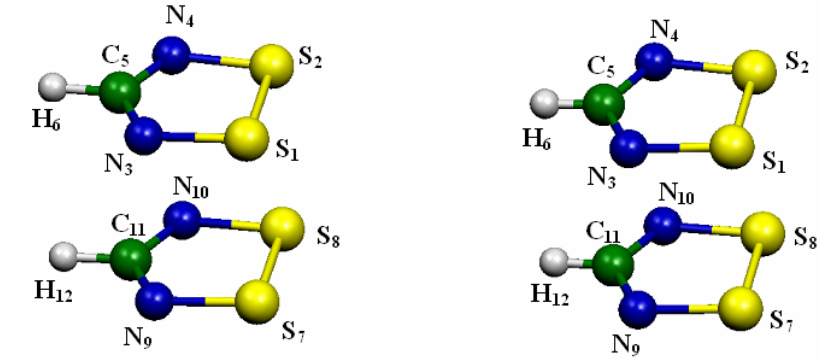

Fig. S5c. Calculated (left) and solid state (right)[13] geometries of $[HCNSSN]_2$ at MPW1PW91/6-31 G* level of theory. Calculated and experimental bond distances and intradimer contacts are listed in table S2.

Table S2. Compilation of experimental and calculated bond dictances of $[ClCNSSS]_2^{2+}$, $[S_3N_2]_2^{2+}$, and $[HCNSSN]_2$.

$[ClCNSSS]_2^{2+}$		
Bond distance, Å	Calculated	Experimental
C(1)-N(5)	1.285	
S(4)-N(5),	1.604	1.615(2)
S(4)-S(3),	2.119	2.0671(8)
S(3)-S(2),	2.047	2.0219(8);
C(1)-S(2),	1.780	1.743(2)
C(1)-Cl(6),	1.673	1.690(2)
intradimer S…S	3.225	3.253(5).
$[S_3N_2]_2^{2+}$		
S(1)-S(2)	2.205	2.145(1)
S(1)-N(1)	1.592	1.613(3)
S(2)-N(2)	1.592	1.613(3)
S(3)-N(1)	1.571	1.569(3)
S(3)-N(2)	1.571	1.566(2)
intradimer S…S	2.990	3.030(1)
$[HCNSSN]_2$		
S(1)-S(2)	2.123	2.065
S(7)-S(8)	2.123	2.066
S(1)-N(3)	1.641	1.643
S(2)-N(4)	1.641	1.634
S(7)-N(9)	1.641	1.637
S(8)-N(10)	1.641	1.638
C(5)-N(3)	1.326	1.330
C(5)-N(4)	1.326	1.323
C(11)-N(10)	1.326	1.299
C(11)-N(9)	1.326	1.337
C(5)-H(6)	1.085	0.952
C(11)-H(12)	1.085	0.945
S(1)-S(7)	3.077	3.113
S(2)-S(8)	3.077	3.107
N(4)-N(10)	3.119	3.161
N(3)-N(9)	3.119	3.108
C(5)-C(11)	3.157	3.106
H(6)-H(12)	3.198	3.061

Table S3. Angular relation between atoms of the dimer and principal axes of *g*-matrix and *D*-tensor (all values are listed in degree, experimental error is 5 degree).

	C_1	N_2	S_3	S_4	S_5	Cl_6
g_{xx}	92	113	121	57	63	93
g_{yy}	22	35	65	73	40	13
g_{zz}	70	67	44	37	65	79
D_{xx}	116	125	105	60	91	123
D_{yy}	128	106	84	126	150	129
D_{zz}	132	142	164	130	121	124

Table S4. Direction cosines between principal axes of *g*-matrix and *D*-tensor.

	D_{xx}	D_{yy}	D_{zz}
g_{xx}	0.611	-0.729	0.309
g_{yy}	-0.635	-0.684	-0.359
g_{zz}	0.473	0.023	-0.881

[8] *Handbook of preparative Inorganic Chemistry*, edited by G. Brauer, vol. 1, p. 663, Academic Press, New York, London, **1963**.
[9] Burford, N.; Passmore, J.; Sanders, J. C. P. *Molecular Structure and Energetics. Isoelectronic Relationships in Atoms to Polymers*, eds. J. F. Liebman and A. G. Greenberg, Verlag Chemie, Deerfield Beach, Florida, **1989**.
[10] Murchie, M. P.; Kapoor, R.; Passmore, J.; Schatte, G. *Inorg. Synth*. **1996**, *31*, 80.
[11] Gaussian 03, Revision C.02, Frisch, M. J.; Trucks, G. W.; Schlegel, H. B.; Scuseria, G. E.; Robb, M. A.; Cheeseman, J. R.; Montgomery, Jr., J. A.; Vreven, T.; Kudin, K. N.; Burant, J. C.; Millam, J. M.; Iyengar, S. S.; Tomasi, J.; Barone, V.; Mennucci, B.; Cossi, M.; Scalmani, G.; Rega, N.; Petersson, G. A.; Nakatsuji, H.; Hada, M.; Ehara, M.; Toyota, K.; Fukuda, R.; Hasegawa, J.; Ishida, M.; Nakajima, T.; Honda, Y.; Kitao, O.; Nakai, H.; Klene, M.; Li, X.; Knox, J. E.; Hratchian, H. P.; Cross, J. B.; Bakken, V.; Adamo, C.; Jaramillo, J.; Gomperts, R.; Stratmann, R. E.; Yazyev, O.; Austin, A. J.; Cammi, R.; Pomelli, C.; Ochterski, J. W.; Ayala, P. Y.; Morokuma, K.; Voth, G. A.; Salvador, P.; Dannenberg, J. J.; Zakrzewski, V. G.; Dapprich, S.; Daniels, A. D.; Strain, M. C.; Farkas, O.; Malick, D. K.; Rabuck, A. D.; Raghavachari, K.; Foresman, J. B.; Ortiz, J. V.; Cui, Q.; Baboul, A. G.; Clifford, S.; Cioslowski, J.; Stefanov, B. B.; Liu, G.; Liashenko, A.; Piskorz, P.; Komaromi, I.; Martin, R. L.; Fox, D. J.; Keith, T.; Al-Laham, M. A.; Peng, C. Y.; Nanayakkara, A.; Challacombe, M.; Gill, P. M. W.; Johnson, B.; Chen, W.; Wong, M. W.; Gonzalez, C.; and Pople, J. A.; Gaussian, Inc., Wallingford CT, 2004.
[12] (a) Flükiger, P.; Lüthi, H. P.; Portmann, S.; Weber, J. MOLEKEL 4.3, Swiss Center for Scientic Computing, Manno (Switzerland), 2000-2002. (b) Portmann, S.; Lüthi, H. P.

MOLEKEL: An Interactive Molecular Graphics Tool. *Chimia* **2000**, *54*, 766-770.
[13] C. D. Bryan, A. W. Cordes, R. C. Haddon, R. G. Hicks, D. K. Kennepohl, C. D. MacKinnon, R. T. Oakley, T. T. M. Palstra, A. S. Perel, S. R. Scott, L. F. Schneemeyer, J. V. Waszczak, *J. Am. Chem. Soc.* **1994**, *116*, 1205.
[14] R. J. Gillespie, J. P. Kent, J. F. Sawyer, *Inorg. Chem.* **1981**, *20*, 3784.